Journal of Power Sources 194 (2009) 668–673

Contents lists available at ScienceDirect

Journal of Power Sources

journal homepage: www.elsevier.com/locate/jpowsour

Carbon nanotubes supported Pt–Au catalysts for methanol-tolerant oxygen reduction reaction: A comparison between Pt/Au and PtAu nanoparticles

Jiajun Wang[a,b], Geping Yin[a,*], Hao Liu[b], Ruying Li[b], Roberta L. Flemming[c], Xueliang Sun[b,**]

[a] School of Chemical Engineering and Technology, Harbin Institute of Technology, Xi Da-zhi Street, Harbin 150001, China
[b] Department of Mechanical and Materials Engineering, The University of Western Ontario, London, Ontario, Canada N6A 5B9
[c] Department of Earth Sciences, The University of Western Ontario, London, Ontario, Canada N6A 5B7

ARTICLE INFO

Article history:
Received 21 April 2009
Received in revised form 15 June 2009
Accepted 16 June 2009
Available online 24 June 2009

Keywords:
Direct methanol fuel cell
Oxygen reduction
Methanol tolerance
Pt–Au nanoparticles

ABSTRACT

Two kinds of Pt–Au/CNT catalysts with different structures are prepared by synthesizing the formerly separated Pt/Au (Au separating Pt) in separate solutions, and PtAu nanoparticles in mixed solution using the borohydride reduction method with trisodium citrate as the stabilizing agent, and then depositing the metal colloid nanoparticles on the carbon nanotubes supporting material. The structural information and particle size are characterized by UV–vis absorption spectra, transmission electron microscopy (TEM), and X-ray diffraction (XRD). The results confirm the formation of Pt–Au nanoparticles with PtAu and separated Pt/Au structures. The catalytic activities for methanol oxidation reaction and oxygen reduction reaction are examined by electrochemical measurements. Compared with the Pt/CNT catalyst, the two Pt–Au/CNT catalysts show a lower overpotential for the oxygen reduction reaction in the presence of methanol, indicating a higher methanol tolerance on Au-modified Pt nanoparticles. Particularly, the Pt/Au/CNT catalyst with Au separating Pt nanoparticles structure exhibits the significantly higher methanol tolerance than PtAu/CNT catalyst. The enhanced methanol tolerance may be attributed to less methanol adsorption on Pt surface due to the effect of Au nanoparticles.

1. Introduction

Direct methanol fuel cells (DMFCs) have been considered to be one of the most promising options for the power source in portable electronic devices due to the high-energy density of methanol, low operating temperature, and ease of handling of liquid fuel [1–3]. Despite the progress, many challenges still remain before commercial application is feasible. One of the important problems is the methanol crossover effect on the cathode electrode [4]. To cope with the problem, one of the solutions is to develop a proton exchange membrane with low methanol permeability [5], and the other method is to employ a methanol-tolerant cathode catalyst [6]. Binary Pt-based catalysts, such as Pt–Ni [7], Pt–Cr [8], and Pt–Fe [9], have been investigated as cathode catalysts for the oxygen reduction reaction, and it was found that these Pt alloy catalysts showed higher methanol tolerance than Pt alone. However, these non-noble elements are easily dissolved during the operation of a DMFC [10,11]. Hence there is great concern in developing methanol-tolerant cathode catalyst with highly stable material.

Au is a good choice because it is more stable under the DMFCs operating conditions. Recently, Adzic and coworkers [12] reported that carbon supported PtAu catalyst exhibited much more stability than carbon supported Pt catalyst. Due to the high stability of Au, its co-catalytic effect in PtAu catalyst for DMFCs has attracted much attention [13,14]. However, there is no any agreement on the co-catalytic effect of Au for methanol oxidation. Some researchers suggested a promoting effect of Au in Pt–Au catalyst for methanol oxidation. Sung and coworkers [15] prepared Pt-modified Au nanoparticles using a successive chemical reduction process and investigated its catalytic activity for methanol. It indicated that Pt-modified Au nanoparticle exhibited higher catalytic activity for methanol oxidation compared to pure Pt nanoparticles, which might be due to the high Pt utilization in the effective surface structure. Sung and coworkers [16] also synthesized PtAu alloy catalyst by the conventional borohydride reduction method and found that this alloy catalyst also showed enhanced activity for methanol oxidation. Baeck and coworkers [17] fabricated mesoporous PtAu alloy film on ITO-coated glass and indicated that this PtAu alloy film showed higher catalytic activity and stability for methanol oxidation compared with a pure Pt electrode. However, some researchers suggested an opposite effect of Au. Rojas and coworkers [18] investigated a series of PtAu/C catalysts and found that the role of Au on the methanol oxidation reaction is negligible when alloyed, thus proposed that Au was used as a component of methanol resistant

* Corresponding author. Tel.: +86 451 86413707; fax: +86 451 86413707.
** Corresponding author. Tel.: +1 519 661 2111x87759; fax: +1 519 661 3020.
E-mail addresses: yingphit@hit.edu.cn (G. Yin), xsun@eng.uwo.ca (X. Sun).

0378-7753/$ – see front matter © 2009 Published by Elsevier B.V.
doi:10.1016/j.jpowsour.2009.06.040

cathode catalyst. Kumar and Phani [19] prepared unalloyed Pt–Au bimetallic nanoparticles by the polyol method and showed that methanol oxidation activity is significantly lowered with increasing content of Au in Pt–Au/C catalyst. The above different results may be due to the different structures and particle sizes of Pt–Au catalyst obtained by different researchers. Clearly, it is necessary to explore the appropriate preparation method to obtain Pt–Au catalyst with different structures, especially for alloyed and unalloyed catalysts, and investigate the effect of Au on Pt catalytic activity for methanol oxidation reaction.

In our earlier study [20], we prepared the Pt/Au/C catalyst by depositing Pt and Au nanoparticles on the carbon support. Pt nanoparticles supported on carbon support were well separated by Au nanoparticles. This novel catalyst shows a high methanol tolerance compared to Pt/C catalyst. In this paper, we prepared formerly separated Pt/Au nanoparticles in separate solutions and PtAu nanoparticles in a mixed solution. Then the two kinds of Pt–Au nanoparticles with different structures but similar particle sizes were deposited on carbon nanotubes by the similar method and the effect of different Pt–Au structures on the catalytic activities for methanol oxidation was investigated. The result was also compared with those obtained with the Pt/CNT catalyst.

2. Experimental

2.1. Catalyst preparation

The two kinds of Pt–Au/CNT catalysts with different structures were prepared by depositing Pt–Au colloids on CNTs support. The carbon nanotubes were synthesized by the floating catalyst chemical vapor deposition method developed in our lab [21]. Prior to the Pt deposition, the carbon nanotubes are modified by means of acidic treatment to remove the metal remains and form more active sites, allowing easier anchoring of the Pt nanoparticles.

A two-step strategy was employed to prepare the two catalysts. The detailed process is shown in Fig. 1. First, the Pt and Au colloids were prepared using methods in the literature [22,23]. The PtAu colloid was obtained by the same method. Then, the deposition process was employed to obtain two catalysts with different structures. The depositing procedures are similar to our previous published paper [20]. Therefore, the two catalysts with the total metal loading (atomic Pt/Au ratio = 1:1) at 40 wt.% were obtained. The separated and alloy-like Pt–Au catalysts were labeled as Pt/Au/CNTs and PtAu/CNTs respectively. For comparison, a 25 wt.% Pt/CNT catalyst was prepared by the similar method, while keeping the mass ratio of Pt to C constant at 25 wt.% with the above two catalysts.

2.2. Electrode preparation

A glass carbon rotating disk electrode was used as a substrate for the catalysts. Prior to test, the electrode was polished with alumina (diameter 0.05 μm) to obtain a mirror finish. A typical suspension of the catalyst ink was prepared by dispersing an amount of the catalyst power in a water–methanol solution (1:1 volume ratio). Then 10 μL of this ink was pipetted onto the surface of the electrode and dried in air at room temperature. After the paste dried, a drop of 5 wt.% Nafion in water solution was spread on the catalyst.

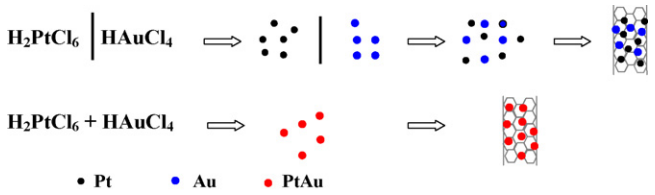

Fig. 1. Schematic illustration for preparation of Pt/Au/CNTs and PtAu/CNT catalysts.

2.3. Instruments and measurements

2.3.1. Electrochemical study

Electrochemical measurements were performed at a standard three-electrode electrochemical cell with CHI 600 C electrochemical working station. A conventional three-electrode cell was used, including an Ag/AgCl (saturated KCl) electrode as the reference electrode, a platinum wire as counter electrode, and a modified glass carbon electrode as the working electrode.

Electrochemical CO stripping voltammograms were measured by oxidation of preadsorbed CO in the 0.5 M H_2SO_4 solution. Before scanning the applied potential, the electrode was held at −0.1 V while CO was purged into the 0.5 M H_2SO_4 solution for 30 min to allow complete adsorption of CO onto the electrode. Excess CO in the electrolyte was then purged out with nitrogen for 30 min. Following the CO adsorption process, cyclic voltammograms between −0.159 V and 0.991 V vs. Ag/AgCl were recorded for each electrode. The amount of CO adsorption was evaluated by integration of the CO stripping peak, corrected by the electric double-layer capacitance. In order to identify the Au cluster on the catalyst, cyclic voltammograms was conducted in the potential between −0.159 V and 1.291 V in the 0.5 M H_2SO_4 solution. Electrocatalytic oxidation of methanol was carried out in 0.5 M CH_3OH + 0.5 M H_2SO_4 solutions by the CV technique (between −0.159 V and +0.991 V) vs. Ag/AgCl at 10 mV s^{-1} at 25 °C. Current-potential relation for oxygen reduction reaction (ORR) in the presence of methanol is measured from −0.1 V to 0.9 V (scan rate 5 mV s^{-1}) to obtain current–potential current in oxygen-saturated 0.5 M CH_3OH + 0.5 M H_2SO_4 solution at 60 °C.

2.3.2. Physical characterization

The metal loadings were determined by inductively coupled plasma-optical emission spectroscopy (ICP-OES). The morphologies and structures of the catalysts were characterized by transmission electron microscopy (TEM) (Philips CM 10) and high-resolution transmission electron microscopy (HRTEM) (JEOL 2010 FEG). Power XRD patterns for the catalysts were obtained on a Bruker D8 Discover Diffractometer using Cu Kα radiation (λ = 1.54056 Å) between 13° and 106° in reflection geometry. UV–vis spectra were collected on an Agilent 8453 UV-Visible Spectrophotometer.

3. Results and discussion

The Pt loadings and metal compositions of the as-prepared catalysts were determined by ICP-OES analysis. The obtained results are found to be very close to the stoichiometric values, indicating that almost all of the metal nanoparticles were deposited on the carbon supports.

The particle size and morphology of the metal nanoparticles were determined using TEM and HRTEM, and typical images are presented in Fig. 2. The low magnification TEM images showed that both kinds of metal nanoparticles are well dispersed on CNTs with little agglomeration (see Fig. 2a and b). Furthermore, the two samples have similar metal dispersion. However, the HRTEM images indicated the remarkable difference between the two kinds of metal nanoparticles (see Fig. 2c and d). With regard to the unsupported Pt/Au nanoparticles (see Fig. 2c), metal nanoparticles with obviously different particle sizes are observed and the bigger ones are ascribed to the Au nanoparticles, which were investigated and characterized in our previous study [20]. Moreover, the HRTEM images consistently showed the lattice planes for the large and small particles with lattice spacings of 0.233 nm and 0.224 nm, respectively,

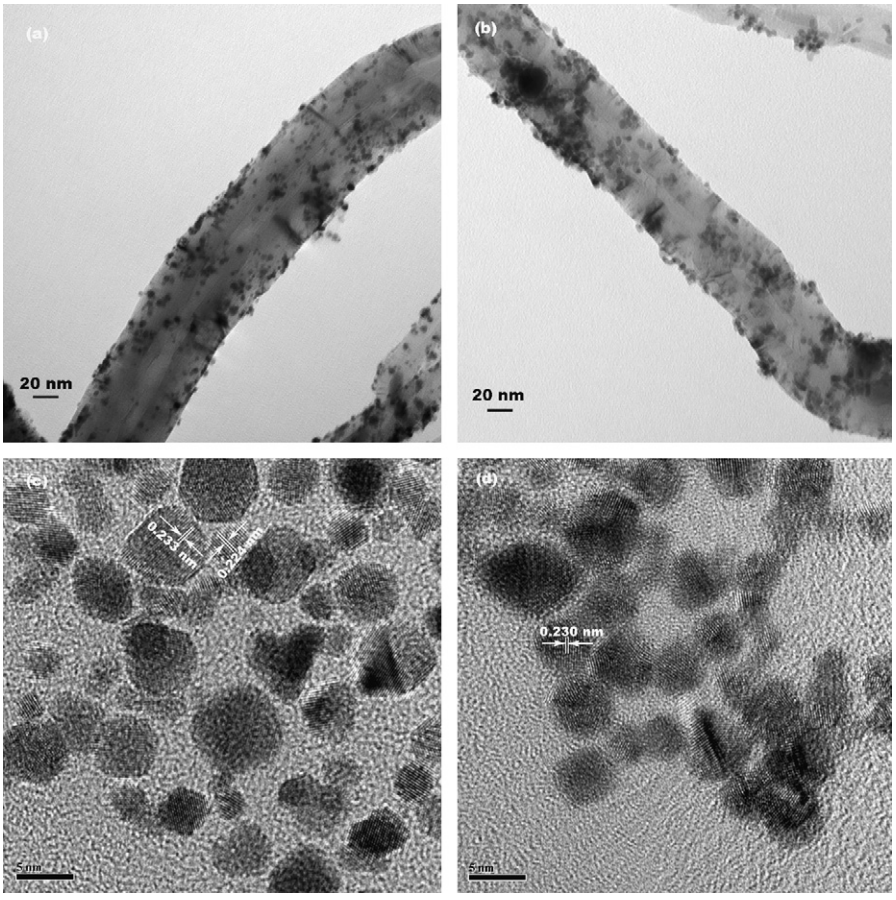

Fig. 2. TEM and HRTEM images of the Pt/Au/CNTs (a), PtAu/CNTs (b) catalysts, Pt/Au (c), and PtAu (d) nanoparticles.

which matches to Au (1 1 1) and Pt (1 1 1) lattice planes [24,25]. The result further confirmed that most of the Pt nanoparticles were separated by the Au nanoparticles. By comparison, unsupported PtAu nanoparticles with uniform particle size can be observed and the size distribution is fairly narrow (see Fig. 2d), which may be due to the effect of alloy-like process. The lattice spacing of 0.230 nm might be due to the presence of the PtAu alloy-like phase. The result is well consistent with the literature [16].

To clearly demonstrate the different structures of the Pt–Au bimetallic catalysts, XRD characterization was employed. Fig. 3 shows the XRD patterns of the Au/CNTs, Pt/CNTs, PtAu/CNTs, and Pt/Au/CNT catalysts. The diffraction patterns for Au/CNTs and Pt/CNTs show a face-centered cubic (fcc) structural characterization. The XRD peak corresponding to the (1 1 1) peak for Au/CNTs is seen at 38.1° and that for Pt/CNTs at 39.1°. The pattern of the PtAu/CNT catalyst exhibited diffraction peaks of (1 1 1), (2 0 0), (2 2 0), and (3 1 1) at 2θ values of 38.5°, 44.7°, 66.0°, and 78.4°, respectively. Compared with that of Pt/CNTs, a smooth peak appears at the (1 1 1) plane in the PtAu/CNT catalyst and an obviously negative shift of the (1 1 1) peak by about 0.6°, which confirms PtAu alloy-like phase formation in the PtAu/CNT catalyst. By contrast, as to the Pt/Au/CNTs, two different peaks appear at the (1 1 1) plane and the sharp peak at 38.0° is attributed to Au and the broad one at around 39.0° corresponds to Pt, indicating that Pt and Au occur at separated phases. The results further demonstrate the presence of the different Pt–Au structures in the two catalysts. The average particle size of the catalyst can be estimated by using the Scherrer's equation [26] according to the previous papers. The calculated particle sizes for Au/CNTs, Pt/CNTs, PtAu/CNTs, and Pt/Au/CNTs are 5.6 nm, 3.7 nm, 3.4 nm, and 3.6 nm respectively.

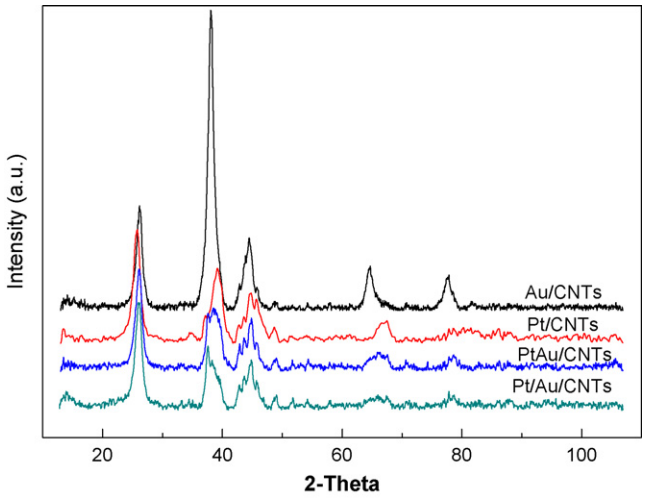

Fig. 3. XRD patterns for Au/CNTs, Pt/CNTs, PtAu/CNTs, and Pt/Au/CNTs.

UV–vis absorption spectra of the metal colloid with different structures and compositions are shown in Fig. 4. The characteristic absorption peak at 511 nm due to the surface plasmon resonance of Au can be clearly observed on Au metal colloids, while no obvious absorption peak appears in Pt nanoparticles, which is well consistent with previous papers [27,28]. For the Pt/Au colloid with separated structure, the density of the Au plasmon absorption peak is decreased and shifted to a higher wavelength. For the PtAu colloid, the Au plasmon absorption peak is almost suppressed completely. The different suppression of Au plasmon absorption peak also further confirms the emergence of different structures for the

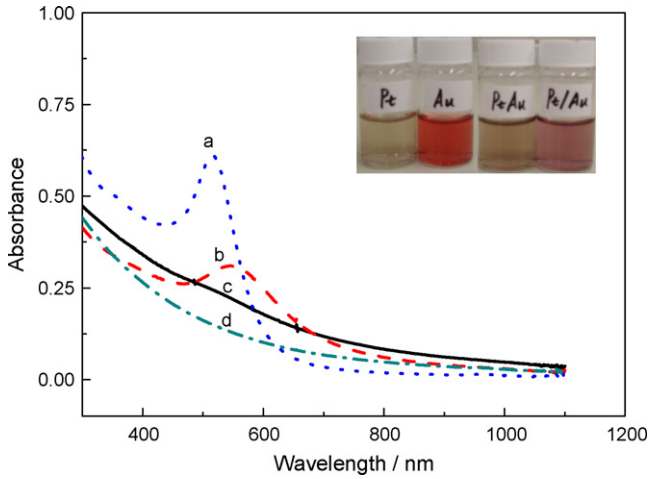

Fig. 4. UV–vis absorption spectra of Au (a), Pt/Au (b), PtAu (c), and Pt (d) colloids.

two kinds of Pt–Au nanoparticles.

The surface structure and composition of metal nanoparticles on carbon nanotube supports are very important because they have a great effect on its catalytic activity. In order to obtain the surface composition and characteristics, cyclic voltammetry of CO stripping on the Pt/Au/CNTs and PtAu/CNT catalysts were performed in 0.5 M H_2SO_4 solutions at a scan rate of 20 mV s^{-1}. For comparison, The Pt/CNT catalyst was also characterized by the same method. Fig. 5 shows the cyclic voltammogram, and the *y*-axis represents the mass specific current density of Pt (mA mg^{-1} Pt). Calculated from the peak areas associated with CO oxidation, the consumed charges upon CO stripping on the Pt/CNTs, Pt/Au/CNTs, and PtAu/CNTs are 258 mC mg^{-1}, 242 mC mg^{-1}, and 156 mC mg^{-1}, respectively. It can be seen that the Pt/Au/CNTs and Pt/CNT catalyst have a similar electrochemical active surface (EAS), which is agrees well with our previous result [20]. Thus, we infer that the Pt nanoparticles in Pt/Au/CNT catalyst were well separated by Au nanoparticles, and Pt surface was not covered by Au nanoparticle, which confirms the observations by HRTEM. By comparison, the PtAu/CNTs show the smaller EAS compared to the other two catalysts, indicating that Pt surface was modified by Au nanoparticle, which might be due to the formation of PtAu colloid during the co-reduction preparation process.

Further experiment was performed by cyclic voltammetry at more positive potentials to probe Au segregation effects. Fig. 6 shows the cyclic voltammetry of the Pt/Au/CNTs and PtAu/CNT catalysts, and the *y*-axis represents the mass specific current density of Au (mA mg^{-1} Au). For comparison, the same experiment was performed at Au/CNT catalyst. As shown in Fig. 6, two reduction peaks appeared at the negative scanning direction and the reduction peaks at 0.7 V and 1.2 V are attributed to the reduction of Pt oxide and Au oxide, respectively. The exposed active surface area of Au on the bimetallic nanoparticles can be compared by the charge corresponding to the stripping of Au surface oxide [15,29]. It is evident that most of Au nanoparticles are exposed and not covered by Pt clusters in the Pt/Au/CNT catalyst. In contrast, in the case of PtAu/CNT catalyst, less Au sites are exposed due to the effect of Pt–Au alloy-like process, thus exhibiting the weak stripping of Au surface oxide. The results further indicate the presence of different structures between the Pt/Au/CNTs and PtAu/CNT catalysts.

The electrocatalytic activities of the above three catalysts were measured by cyclic voltammetry in 0.5 M CH_3OH + 0.5 M H_2SO_4 solution. The reported current density was normalized by the mass specific activity of Pt. As shown in Fig. 7, compared with the Pt/CNT catalyst, the PtAu/CNTs and Pt/Au/CNT catalysts both show lower current density, indicating that the presence of Au in the Pt catalyst will decrease the catalytic activity for methanol oxidation reaction. Moreover, the Pt/Au/CNT catalyst with separated structure shows the lowest activity for methanol oxidation. It should be noted that the as-prepared PtAu/CNT catalyst might have a low alloy-like extent because the synthesis process is performed by solution method at low temperature. The alloyed extent may be

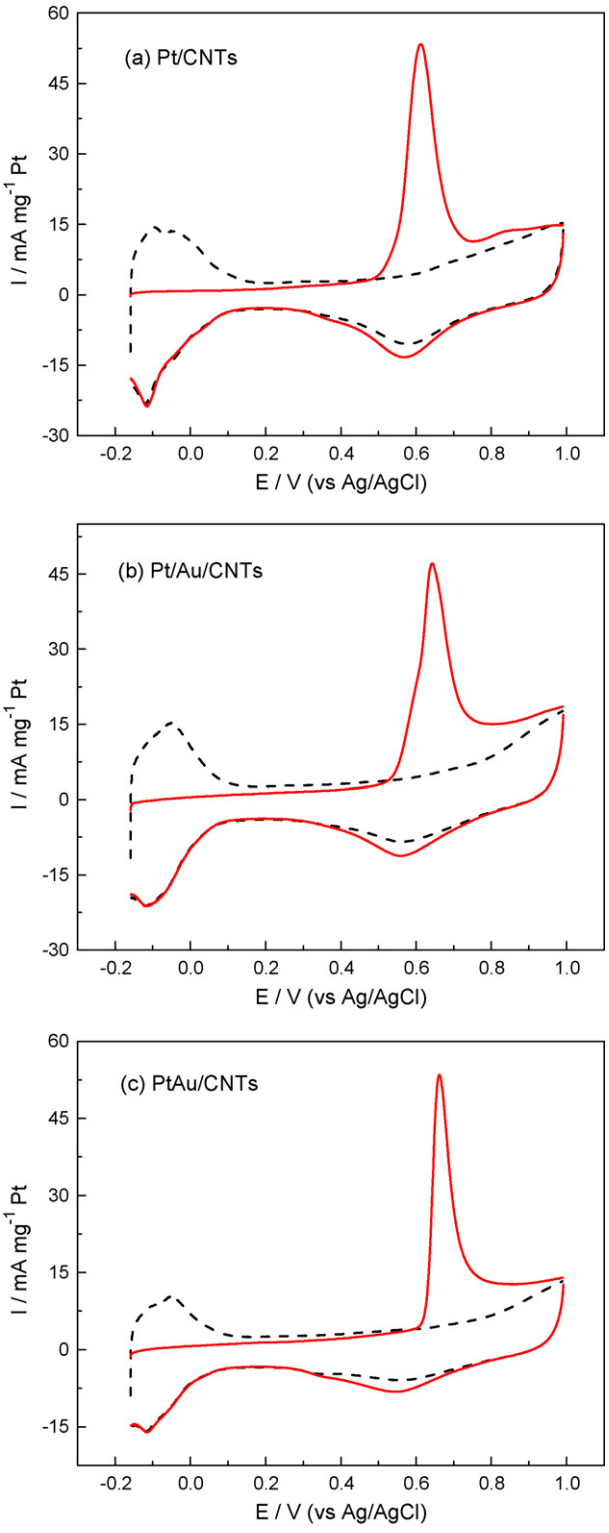

Fig. 5. Cyclic voltammograms of CO stripping on the Pt/CNTs, Pt/Au/CNTs, and PtAu/CNT catalysts in 0.5 M H_2SO_4. Dash curves were CVs for the electrodes without CO adsorption.

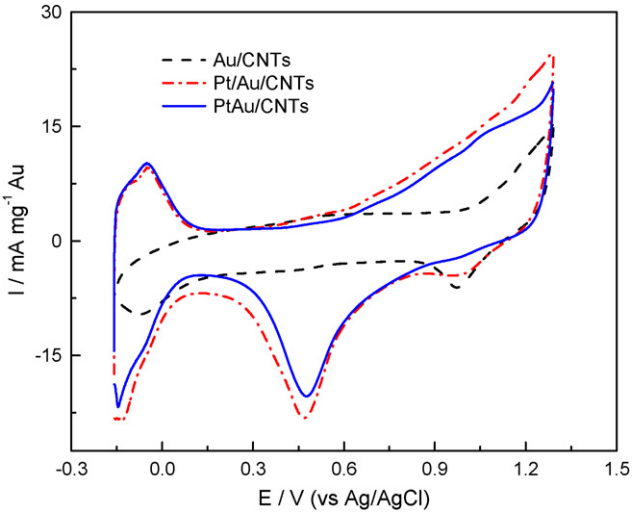

Fig. 6. Cyclic voltammograms of the Pt/Au/CNTs, PtAu/CNTs, and Au/CNT catalysts recorded in 0.5 M H_2SO_4 solution at a scan rate of 20 mV s^{-1}.

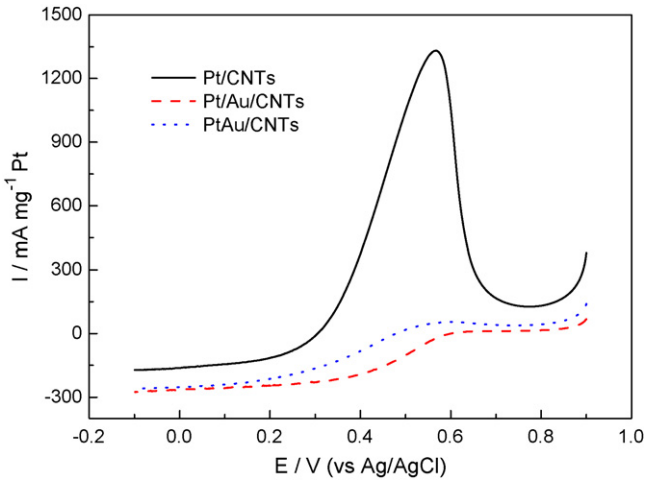

Fig. 8. Linear scan voltammograms of the Pt/Au/CNTs, PtAu/CNTs, and Pt/CNT catalysts recorded in 0.5 M H_2SO_4 solution containing 0.5 M CH_3OH saturated with pure oxygen at a scan rate of 5 mV s^{-1} and a rotation speed of 3200 rpm.

easily increased by heat-treatment or other preparation methods at high temperature; however, this would have the effect of increasing the particle [30]. Thus, the comparison between the Pt–Au catalysts with different particle sizes is not reasonable because the particle size has a great effect on the catalytic activity for methanol oxidation reaction [31]. The advantage of the method discussed here is the ability to obtain Pt–Au nanoparticles with significantly different alloyed and separated (unalloyed) structures, while keeping the particle size similar for the two catalysts. Thus, it is plausible to get more accurate information about the effect of Au on Pt nanoparticles for catalytic activity for methanol oxidation reaction.

In our previous study, this Pt/Au separating structure on Vulcan XC-72 showed a higher catalytic activity for oxygen reduction reaction. Enhancement of the activity of Pt catalyst for oxygen reduction reaction by Au nanoparticles has been reported by Kumar and Phani [19] in a recent study. Thus, this Au-modified Pt catalyst can be used as a more promising methanol resistant cathode catalyst for DMFC. For further simulating the working condition of DMFC, the response of the ORR in the presence of methanol on the three catalysts was obtained from linear voltammetry experiments in 0.5 M CH_3OH + 0.5 M H_2SO_4 solution at 60 °C. Fig. 8 shows the results obtained for the three catalyst samples. From the curve of Pt/CNT catalyst, it can be seen that a significantly high methanol oxidation peak appeared during the ORR process; thus there is a significant increase in the overpotential of the ORR. The significant increase in the overpotential of the oxygen reduction reaction is due to the competitive reaction between oxygen reduction and methanol oxidation, especially for Pt/CNT catalyst. Compared with Pt/CNTs, the Au-modified Pt catalysts show a low methanol oxidation peak, thus the Pt/Au/CNTs and PtAu/CNTs still exhibit a high catalytic activity for ORR in the presence of methanol. Among the three catalysts, the methanol oxidation current on Pt/Au/C catalyst is negligible, indicating the highest methanol tolerance. Thus, the Au-modified Pt nanoparticles show a high methanol tolerance, and in particular the Pt/Au nanoparticles with separated or unalloyed structure are more promising.

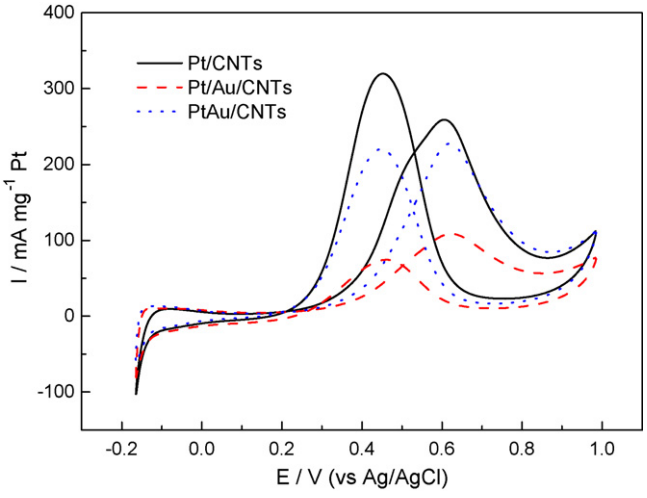

Fig. 7. Cyclic voltammograms of the Pt/Au/CNTs, PtAu/CNTs, and Pt/CNT catalysts recorded in 0.5 M H_2SO_4 solution containing 0.5 M CH_3OH at a scan rate of 10 mV s^{-1}.

It is well established that at least three adjacent Pt active sites in a proper crystallographic orientation are necessary to initiate the chemisorption of methanol [32–35]. In the two kinds of Au-modified Pt catalysts, the Pt/Au ration is 1.0 and the probability of finding three neighboring Pt active sites on the surface is lower than the Pt/CNT catalyst. Also, it is well known that Au itself is not active to methanol oxidation reaction, so the presence of methanol-tolerant Au around Pt active sites could hinder methanol adsorption on Pt sites due to the dilution effect, which suppresses methanol oxidation on the Au-modified Pt catalyst. Therefore, the both Pt/Au/CNTs and PtAu/CNT catalysts show higher methanol tolerance than Pt/CNTs. Besides, in this study, the Pt/Au/CNT catalyst exhibits higher methanol tolerance compared with that of PtAu/CNT catalyst. This might be explained as follows. In addition to the dilution effect for Pt active sites mentioned above, Au may have another effect on Pt nanoparticles by electronic modification. The electronic modifying effect of Au may enhance the catalytic activity of Pt nanoparticles for methanol oxidation reaction [36], which is opposite to the result of Au dilution effect. In the case of PtAu/CNT catalyst, the above two opposing effects may occur simultaneously. By comparison, Pt nanoparticles in Pt/Au/CNT catalyst may be affected only by the Au nanoparticles dilution due to the separated or unalloyed structure. Hence, the Pt/Au/CNT catalyst exhibited the higher methanol tolerance than PtAu/CNT catalyst.

4. Conclusions

Two kinds of Pt–Au/CNTs were prepared by a two-step method using KBH_4 and trisodium citrate as the reducing and stabilizing agents, respectively. Uniform Pt/Au separated and PtAu

nanoparticles were obtained by this simple method. Electrochemical measurement indicated that the presence of Au enhanced the methanol tolerance of Pt in the oxygen reduction reaction, whether using an alloy-like or separated Pt–Au structure. Moreover, the Pt/Au/CNT catalyst with separated Pt–Au structure shows the highest activity for ORR in the methanol-containing electrolyte. This result may be due to the low methanol absorption and the Au dilution effect. The novel Pt/Au/CNT catalyst may serve as an efficient methanol-tolerant cathode catalyst in DMFCs.

Acknowledgement

We are in debt to David Tweddell for his kind help and fruitful discussions.

References

[1] B.D. McNicol, D.A.J. Rand, K.R. Williams, J. Power Sources 83 (1999) 15–31.
[2] V.M. Barragan, A. Heinzel, J. Power Sources 104 (2002) 66–72.
[3] S. Surampudi, S.R. Narayanan, E. Vamos, H. Frank, G. Halpert, A. LaConti, J. Power Sources 47 (1994) 377–385.
[4] T.H. Kim, Y.C. Bae, Polymer 46 (2005) 6494–6499.
[5] M. Bello, S.M. Javaid Zaidi, S.U. Rahman, J. Membr. Sci. 322 (2008) 218–224.
[6] R.W. Reeve, P.A. Christensen, A.J. Dickinson, A. Hamnett, K. Scott, Electrochim. Acta 45 (2000) 4237–4250.
[7] E. Antolini, J.R.C. Salgado, E.R. Gonzalez, J. Electroanal. Chem. 580 (2005) 145–154.
[8] H. Yang, N. Alonso-Vante, J.M. Leger, C. Lamy, J. Phys. Chem. B 108 (2004) 1938–1948.
[9] L. Xiong, A. Manthiram, Electrochim. Acta 49 (2004) 4163–4170.
[10] P. Yu, M. Pemberton, Paul Plasse, J. Power Sources 144 (2005) 11–20.
[11] J.R.C. Salgado, E. Antolini, E.R. Gonzalez, J. Power Sources 141 (2005) 13–18.
[12] J. Zhang, K. Sasaki, E. Sutter, R.R. Adzic, Science 315 (2007) 220–222.
[13] Y. Gohda, A. Groß, J. Electroanal. Chem. 607 (2007) 47–53.
[14] Y. Yu, Y. Hu, X. Liu, W. Deng, X. Wang, Electrochim. Acta 54 (2009) 3092–3097.
[15] I.S. Park, K.S. Lee, D.S. Jung, H.Y. Park, Y.E. Sung, Electrochim. Acta 52 (2007) 5599–5605.
[16] J.H. Choi, K.W. Park, I.S. Park, K. Kim, J.S. Lee, Y.E. Sung, J. Electrochem. Soc. 153 (2006) A1812–A1817.
[17] E.K. Park, J.K. Lee, Y.S. Kim, G.P. Kim, S.H. Baeck, Fuel Cell Bull. 6 (2008) 12–14.
[18] P. Hernandez Fernandez, S. Rojas, P. Ocon, A. de Frutos, J.M. Figueroa, P. Terreros, M.A. Pena, J.L.G. Fierro, J. Power Sources 177 (2008) 9–16.
[19] S.S. Kumar, K.L.N. Phani, J. Power Sources 187 (2009) 19–24.
[20] J.J. Wang, G.P. Yin, G.J. Wang, Z.B. Wang, Y.Z. Gao, Electrochem. Commun. 10 (2008) 831–834.
[21] Y. Zhang, R.Y. Li, H. Liu, X.L. Sun, P. Mérel, S. Désilets, Appl. Surf. Sci. 255 (2009) 5003–5008.
[22] Y.D. Jin, Y. Shen, S.J. Dong, J. Phys. Chem. B 108 (2004) 8142–8150.
[23] K.C. Grabar, K.J. Allison, B.E. Baker, R.M. Bright, K.R. Brown, R.G. Freeman, A.P. Fox, C.D. Keating, M.D. Musick, M.J. Natan, Langmuir 12 (1996) 2353–2361.
[24] A. Chu, J. Cook, R.J.R. Heesom, J.L. Hutchison, M.L.H. Green, J. Sloan, Chem. Mater. 8 (1996) 2751–2754.
[25] J.H. He, E. Muto, T. Kunitake, S.X. Liu, S. Zhang, X.M. Liu, Chem. Phys. Lett. 454 (2008) 274–278.
[26] J.B. Xu, T.S. Zhao, Z.X. Liang, J. Power Sources 185 (2008) 857–861.
[27] X.W. Teng, W.Q. Han, Q. Wang, L. Li, A.I. Frenkel, J.C. Yang, J. Phys. Chem. 112 (2008) 14696–14701.
[28] N. Kristian, X. Wang, Electrochem. Commun. 10 (2008) 12–15.
[29] S. Papadimitriou, A. Tegoua, E. Pavlidou, S. Armyanov, E. Valova, G. Kokkinidis, S. Sotiropoulos, Electrochim. Acta 53 (2008) 6559–6567.
[30] E. Ding, K.L. More, T. He, J. Power Sources 175 (2008) 794–799.
[31] O.V. Cherstiouk, P.A. Simonov, E.R. Savinova, Electrochim. Acta 48 (2003) 3851–3860.
[32] C. Lamy, A. Lima, V.Le. Rhun, C. Countanceau, J.M. Leger, J. Power Sources 105 (2002) 283–296.
[33] H.A. Gasteiger, N.M. Markovic, P.N. Ross, E.J. Cairns, Electrochim. Acta 39 (1994) 1825–1832.
[34] H.A. Gasteiger, N. Markovic, P.N. Ross, E.J. Cairns, J. Electrochem. Soc. 141 (1994) 1795–1803.
[35] N.M. Markovic, P.N. Ross, Surf. Sci. Rep. 45 (2002) 117–229.
[36] E. Antolini, Mater. Chem. Phys. 78 (2003) 563–573.